Advances in Applied Mathematics and Mechanics
Adv. Appl. Math. Mech., Vol. **16**, No. 2, pp. 398-422

DOI: 10.4208/aamm.OA-2021-0289
April 2024

An Analytical Approach for Buckling of FG Cylindrical Nanopanels Resting on Pasternak's Foundations in the Thermal Environment

Do Quang Chan[1,2,*], Bui Gia Phi[3], Nguyen Thi Thu Nga[3], Minh-Quy Le[4] and Van-Hieu Dang[5]

[1] *Faculty of Mechanical Engineering and Mechatronics, Phenikaa University, Hanoi 12116, Vietnam*
[2] *Phenikaa Research and Technology Institute (PRATI), A&A Green Phoenix Group JSC, No. 167 Hoang Ngan, Trung Hoa, Cau Giay, Hanoi 11313, Vietnam*
[3] *Faculty of Technical Fundamental, University of Transport Technology, 54 Trieu Khuc, Thanh Xuan, Hanoi, Vietnam*
[4] *School of Mechanical Engineering, Hanoi University of Science and Technology, No. 1, Dai Co Viet Road, Hanoi, Vietnam*
[5] *Department of Mechanics, Thainguyen University of Technology, 666, 3/2 street, Tich Luong Ward, Thai Nguyen City, Thainguyen, Vietnam*

Received 9 September 2021; Accepted (in revised version) 29 August 2022

Abstract. In this article, the effects of temperature and size-dependent on the buckling behavior of functionally graded (FG) cylindrical nanopanels resting on elastic foundation using nonlocal strain gradient theory are investigated in detail analytical approach. According to a simple power-law distribution, the material properties of FG cylindrical nanopanels are assumed to vary continuously through the thickness direction. The Pasternak model is used to describe the reaction of the elastic foundation on the FG cylindrical nanopanels. The fundamental relations and stability equations are derived by applying the nonlocal strain gradient theory and the classical shell theory based on the adjacent equilibrium criterion. Using Galerkin's method, the mechanical buckling behavior of FG cylindrical nanopanels resting on an elastic foundation in the thermal environment is solved. The reliability of the obtained results has been verified by comparison with the previous results in the literature. Based on the obtained results, the influences of the material length scale parameter, the nonlocal parameter, temperature increment, geometric parameters, material properties, and elastic foundation on buckling behaviors of FG cylindrical nanopanels resting on an elastic foundation in the thermal environment are analyzed and discussed.

AMS subject classifications: 74K25, 74G60

Key words: Functionally graded materials, cylindrical nanopanel, nonlocal strain gradient theory, thermal, Galerkin method.

---

*Corresponding author.
Email: chan.doquang@phenikaa-uni.edu.vn (D. Chan)

1 Introduction

Functionally graded materials (FGMs) are a new generation of engineering materials proposed in 1984 by Japanese researchers. FGMs are usually composed of ceramic and metal so that material properties vary smoothly and continuously through the thickness from the surface to the other surface. The mechanical properties are graded in the thickness direction according to volume fraction power-law distribution, exponential distribution, or sigmoid distribution. The importance of FGMs was realized by popular applications in many fields such as tanks and pressure vessels, missiles and spacecraft, submarines, nuclear reactors, jet nozzles, and aerospace engineering structures, more and more studies focused on buckling, vibration, and dynamic responses of FGMs structures [1–4].

Nowadays, because of the brilliant properties such as mechanical properties, electrical properties, thermal properties, and other known physical and chemical properties, the nanoscale structures consist of functionally graded (FG) nanoscale structures are becoming to increase used in different fields of science and technology such as engineering, medicine, aerospace, electronics, and modern industry. Mechanical behaviors, including vibration, buckling, static deformation, and dynamic response, have a significant role in the overall operation of many nanoelectromechanical systems. For nanoscale structures, the material properties can vary from one point to another. Studying the behavior of nanoscale structures using classical theories is inaccurate because these theories ignore the size dependence and inability to describe the effects of the nanostructures size. Therefore, several size-dependent continuum theories have been proposed that could observe the size-dependent effect on the static and dynamic responses of nanoscale structures such as the nonlocal elasticity theory [5, 6], the surface elasticity [7–9], the couple stress and modified couple stress theories [10–14]. Besides, the Doublet Mechanics theory [15–17] and Energy equivalent methods [18–20] have been used to analyze stability, dynamic, and vibration of carbon nanotubes. Recently, by incorporating the effects of strain gradients and stress nonlocalities in one continuum-based theory, Lim et al. proposed the nonlocal strain gradient theory [21]. This theory can be considered to be the most generalized elasticity theory to date. This elasticity theory takes the advantages of pure nonlocal and strain gradient models, leading to a higher-order size-dependent model which can be used for a wide range of small size structure types.

Several researchers have investigated several works related to the mechanical behaviors of FG nanoscale structures using the above continuum-based models. Based on Eringen's nonlocal elasticity and Euler–Bernoulli beam theory, Ghadiriat et al. [22] presented a free vibration analysis of size-dependent FG rotating nanobeams with all surface effect considerations. The nonlinear free vibration analysis of nonlocal strain gradient nanobeams has been presented by Şimşek [23]. In this paper, the nanobeam's material properties are assumed to vary continuously in the thickness direction according to simple power-law. The basic equations and the motion equations are derivered using the nonlocal strain gradient theory and Euler-Bernoulli beam theory in conjunction with Hamilton's principle and Galerkin's approach. Mehralian and Beni [24] investigated the size-dependent free vibration of shear deformable FG nanotubes based on the nonlocal strain gradient theory and Hamilton's principle. Abdelrahman et al. [25] analyzed the dynamic behavior of the perforated Reddy nanobeam under moving load using the nonlocal strain gradient theory. The kinematic assumption of the third order shear deformation beam theory in conjunction with nonlocal strain gradient elastic theory are proposed to derive the equation of motion of nanobeam. Based on the virtual work principle, the governing equations of motion of perforated Reddy nanobeams are derived and these equations are solved by Navier's approach. The free vibration and dynamic response of sigmoid/symmetric FG nanobeams under moving load were investigated by Esen et al. [26]. In this study, the FG Timoshenko beam model was developed in the framework of nonlocal strain gradient theory. The Hamilton principle is employed to drive the dynamic equations of motion. An analytical solution methodology for free and forced vibration problems was developed based on Navier's approach. Chen et al. [27] presented the nonlinear vibration, and post-buckling of multilayer FG graphene reinforced porous nanocomposite beams based on the Halpin-Tsai micro-mechanics model. Attia [28] studied size-dependent bending, buckling, and free vibration responses of FG nanobeams by incorporating Eringen's nonlocal elasticity theory, modified couple stress theory, and surface elasticity theory the classical Euler–Bernoulli beam model. Arefi et al. studied the bending of FG nano-beam [29] and sandwich nanobeams [30] in thermal, mechanical, electrical, and magnetic environments based on Eringen's nonlocal elasticity theory. Arefi and Zenkour [31] presented wave propagation analysis of an FG magneto-electro-elastic nanobeam resting on the visco-Pasternak foundation and considering surface elasticity effects. Post-buckling and thermal post-buckling analysis of imperfect nanobeams considering surface effects were investigated by Barati and Zenkour [32, 33]. Ebrahimi and Salari [34] investigated thermal effects on buckling and free vibration behaviors of FG size-dependent nanobeams subjected to various thermal loading types by presenting a Navier type solution. Based on Eringen's nonlocal elasticity theory, modified couple stress theory, and nonlocal strain gradient elasticity theory, Ebrahimi and Barati analyzed the vibration of FG nanobeams [35, 36] and buckling response of size-dependent shear-deformable curved FG nanobeams [37].

The static and dynamic behaviors of the FG nanopanels are also interested in research. Zenkour and Arefi [38] reported the transient thermo-electro-mechanical vibration and bending analysis of an FG piezoelectric nanosheet resting on visco-Pasternak's foundation and subjected to mechanical, thermal, and electrical loadings using the nonlocal elasticity theory as well as classical plate theory and Hamilton's principle. Based on the modified couple stress theory and Hamilton's principle, the size-dependent vibration behavior of FG rectangular Mindlin microplates, including geometrical nonlinearity, was investigated by Ansari et al. [39]. Kolahchi et al. [40] studied nonlinear buckling of embedded polymeric temperature-dependent single-walled carbon nanotubes-reinforced microplates resting on an elastic matrix as an orthotropic temperature-dependent elastomeric medium using Eringen's nonlocal elasticity theory. Also, the size-dependent thermal stability analysis of embedded FG annular nanopanels resting on an elastic foundation was presented by Ashoori et al. [41]. Daikh et al. [42] presented the bending deflection and stress distribution of sandwich functionally graded nanoplates rested on variable Winkler elastic foundation based on new quasi 3D hyperbolic shear theory in conjoint with nonlocal strain gradient theory. New 3D hyperbolic shear theory is exploited to satisfy parabolic variation of shear through thickness direction and zero shear at the bottom and top surfaces. The comprehensive model and governing equilibrium equations of SFG nanoplates is derived in detail with principle of virtual work and solved analytically by Galerkin method. Ebrahimi and Heidari [43] investigated surface effects on nonlinear vibration of embedded FG nanopanels resting on a Pasternak linear elastic foundation based on the third-order shear deformation plate theory and von Karman nonlinearity in conjunction with Gurtin–Murdoch surface continuum theory. Using the nonlocal strain gradient theory, the vibration of FG piezoelectric nanopanels [44] and effects of hygro-thermal, electromagnetic on buckling, vibration and wave propagation in nanopanels were also investigated in [45, 46].

Besides the problems related to FG nanobeams and nanopanels, FG nanoshells' mechanical responses have been considered by using advanced continuum elasticity theories. Barati [47] studied the free vibrational behavior of porous FG nanoshells via the first-order shear deformation theory and the nonlocal strain gradient theory. Arefi et al. [48] presented the bending response of FG composite doubly curved nanoshells with thickness stretching resting on an elastic foundation via the higher-order sinusoidal shear theory. Sahmani and his co-workers presented small scale effects on buckling and postbuckling behaviors of axially loaded hybrid FG and FG nanoshells using the nonlocal elasticity theory [49] and the nonlocal strain gradient elasticity theory [50, 51]. Lu et al. [52] developed a novel size-dependent FG cylindrical shell model based on the nonlocal strain gradient theory in conjunction with the Gurtin-Murdoch surface elasticity theory. Based on the nonlocal elasticity theory, Arefi and Zenkour [53] investigated two-dimensional thermoelastic analysis of an FG nanoshell in frameworks the first-order shear deformation theory. Liu and Wang [54] studied free vibration of FG piezoelectric material cylindrical nanoshells with porosites under thermo-electro-mechanical loading in considering small scale effect according to the Love's shell theory and the nonlocal elasticity theory. Also, Zhang and Zhang [55] investigated free vibration and buckling responses of FG nanoporous metal foam nanoshells by using the first-order shear deformation shell theory and Mindlin's most general strain gradient theory.

The overviews above show few studies related to the bending, buckling, and vibration behaviors of FG cylindrical nanoshell structures based on the nonlocal strain gradient theory. It is noted that previous papers have not considered the effects of the thermal environment, elastic foundation, and size-dependent effect on the static and dynamic behaviors of FG cylindrical nanopanels. So, this study is carried out to fill this gap in analysis of sandwich panel. The novelty of this paper considers the effects of size-dependent, thermal increment, and elastic foundation on buckling characteristics of FG cylindrical nanopanles based on the nonlocal strain gradient theory. It is assumed that the FG cylindrical nanopanel is subjected axial compression in thermal environment. The properties of FG material nanopanel is assumed to vary along the thickness direction power-law expression. The fundamental relations and stability equations are derived by applying the nonlocal strain gradient theory and the classical shell theory based on the adjacent equilibrium criterion. Using Galerkin's method, the mechanical buckling behavior of FG cylindrical nanopanels resting on an elastic foundation in the thermal environment is solved. Moreover, the numerical results indicate that the nonlocal parameter and strain gradient parameter, the geometric parameters, material properties, elastic foundation, and thermal environment have essential roles in the buckling behavior of FG nano cylindrical panels.

2 Fundamental relations

Here, a cylindrical nanopanel is considered with uniform thickness h, mean radius R, span angle θ_0 and length of straight edge L, curved edge $b=R\theta_0$. The cylindrical coordinate system $(x,\, y=R\theta,\, z)$ is chosen such that the x and y axes are in the longitudinal and circumferential directions, respectively, and the z-axial is perpendicular to the middle surface and in the inward thickness direction $(-h/2\le z\le h/2)$ as illustrated in Fig. 1.

The cylindrical nanopanel is made of functionally graded materials in which the volume fractions of ceramic and metal are assumed to vary along the thickness direction of the plate as [51,58]

$$V_c(z)=\left(\frac{2z+h}{2h}\right)^k, \quad V_m(z)=1-V_c(z), \tag{2.1}$$

where, subscripts m and c denote for the metal and ceramic constituents, respectively; k is volume fraction index $(0\le k<\infty)$.

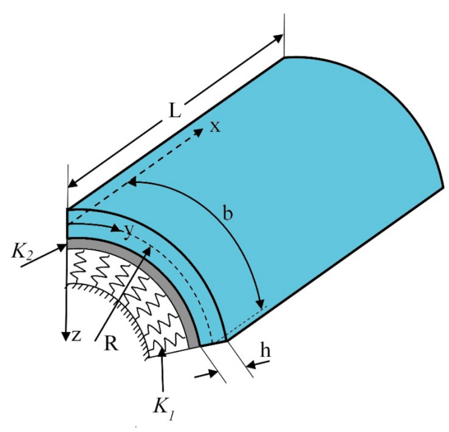

Figure 1: Geometry of cylindrical nanopanel resting on elastic foundation.

From Eq. (2.1), the elasticity modulus (E) and thermal expansion coefficient (α) of the FG nanopanel is given by [58]:

$$E(z)=E_m(z)+[E_c(z)-E_m(z)]\left(\frac{2z+h}{2h}\right)^k, \tag{2.2a}$$

$$\alpha(z)=\alpha_m(z)+[\alpha_c(z)-\alpha_m(z)]\left(\frac{2z+h}{2h}\right)^k, \tag{2.2b}$$

where E_c and E_m are elasticity modulus of ceramic and metal, and α_c, α_m are the thermal expansion coefficient of ceramic and metal, respectively.

The Pasternak model is used to describe the reaction of the elastic foundation on the FG cylindrical nanopanles. The plate-foundation interaction is represented by the Pasternak model as [58]:

$$q_f(x,y)=K_1w-K_2\left(\frac{\partial^2 w}{\partial x^2}+\frac{\partial^2 w}{\partial y^2}\right), \tag{2.3}$$

in which, q_f is the foundation interface pressure, w is the deflection of the shell, K_1 and K_2 are the Winkler foundation modulus and the shear layer foundation stiffness of the Pasternak model, respectively.

The nonlocal strain gradient theory considers both the nonlocal elastic stress field and the strain gradient stress field by introducing two scale parameters. According to this theory, the constitutive relationship corresponding to the total nonlocal strain gradient stress tensor considering thermal effects is given by the following simplicity form [41,45, 50]

$$\left[1-\mu^2\nabla^2\right]\sigma_{ij}=\left(1-l^2\nabla^2\right)\left(C_{ijkl}\varepsilon_{kl}-\alpha_{ij}\Delta T\right), \tag{2.4}$$

where $\mu=ea$ represents the nonlocal parameter, α_{ij} are the thermal expansion coefficients; ΔT is the temperature change.

In this article, the classical shell model has been considered. The strain–displacement relationship at the middle surface and the curvatures, twist of the FG cylindrical nanopanels with the von-Kármán geometrical nonlinearity are given by [47,57,58]:

$$\varepsilon_x^0=u_{,x}+\frac{1}{2}w_{,x}^2,\quad \varepsilon_y^0=v_{,y}-\frac{w}{R}+\frac{1}{2}w_{,y}^2, \tag{2.5a}$$

$$\gamma_{xy}^0=u_{,y}+v_{,x}+w_{,x}w_{,y}, \tag{2.5b}$$

$$\chi_x=-w_{,xx},\quad \chi_y=-w_{,yy},\quad \chi_{xy}=-w_{,xy}, \tag{2.5c}$$

where $y=R\theta$, subscript $(,)$ indicates partial derivative; u, v, w are the displacement components in the x, y, z coordinate directions, respectively; ε_x^0 and ε_y^0 are the normal strains, γ_{xy}^0 is the shear strain, and χ_x, χ_y and χ_{xy} are the change of curvatures and twist, respectively.

The strain components at a distance z from the middle surface of the FG cylindrical nanopanels are given by:

$$\varepsilon_x=\varepsilon_x^0+z\chi_x,\quad \varepsilon_y=\varepsilon_y^0+z\chi_y,\quad \gamma_{xy}=\gamma_{xy}^0+2z\chi_{xy}. \tag{2.6}$$

The stress-strain relations, including temperature effects and the force and the moment resultants of the FG cylindrical nanopanels can be determined by [47,54,58]

$$\sigma_x=\frac{E(z)}{1-\nu^2}\left(\varepsilon_x+\nu\varepsilon_y\right)-\frac{E(z)\alpha(z)\Delta T(z)}{1-\nu},\quad \sigma_y=\frac{E(z)}{1-\nu^2}\left(\varepsilon_y+\nu\varepsilon_x\right)-\frac{E(z)\alpha(z)\Delta T(z)}{1-\nu}, \tag{2.7a}$$

$$\sigma_{xy}=\frac{E(z)}{2(1+\nu)}\gamma_{xy},\left(N_x,N_y,N_{xy}\right)=\int_{-\frac{h}{2}}^{\frac{h}{2}}\left(\sigma_x,\sigma_y,\sigma_{xy}\right)dz, \tag{2.7b}$$

$$\left(M_x,M_y,M_{xy}\right)=\int_{-\frac{h}{2}}^{\frac{h}{2}}\left(\sigma_x,\sigma_y,\sigma_{xy}\right)zdz, \tag{2.7c}$$

where ΔT denotes the change of environment temperature from a stress-free initial state.

Setting Eqs. (2.5)-(2.7a) only with the linear form of the strains and curvatures, and twist in terms of the displacement components into Eq. (2.7b), the constitutive relations for the FG cylindrical nanopanels based on the nonlocal strain gradient theory can be expressed as:

$$\left(1-\mu^2\nabla^2\right)N_x=\left(1-l^2\nabla^2\right)\left[A_{11}\frac{\partial u}{\partial x}+A_{12}\left(\frac{\partial v}{\partial y}-\frac{w}{R}\right)-B_{11}\frac{\partial^2 w}{\partial x^2}-B_{12}\frac{\partial^2 w}{\partial y^2}+T_1\right], \tag{2.8a}$$

$$\left(1-\mu^2\nabla^2\right)N_y=\left(1-l^2\nabla^2\right)\left[A_{21}\frac{\partial u}{\partial x}+A_{22}\left(\frac{\partial v}{\partial y}-\frac{w}{R}\right)-B_{21}\frac{\partial^2 w}{\partial x^2}-B_{22}\frac{\partial^2 w}{\partial y^2}+T_1\right], \tag{2.8b}$$

$$\left(1-\mu^2\nabla^2\right)N_{xy}=\left(1-l^2\nabla^2\right)\left[A_{33}\left(\frac{\partial u}{\partial y}+\frac{\partial v}{\partial x}\right)-B_{33}\frac{\partial^2 w}{\partial x\partial y}\right], \tag{2.8c}$$

$$\left(1-\mu^2\nabla^2\right)M_x=\left(1-l^2\nabla^2\right)\left[B_{11}\frac{\partial u}{\partial x}+B_{12}\left(\frac{\partial v}{\partial y}-\frac{w}{R}\right)-D_{11}\frac{\partial^2 w}{\partial x^2}-D_{12}\frac{\partial^2 w}{\partial y^2}+T_2\right], \tag{2.8d}$$

$$\begin{aligned}\left(1-\mu^2\nabla^2\right)M_y=\left(1-l^2\nabla^2\right)\left[B_{21}\frac{\partial u}{\partial x}+B_{22}\left(\frac{\partial v}{\partial y}-\frac{w}{R}\right)-D_{21}\frac{\partial^2 w}{\partial x^2}-D_{22}\frac{\partial^2 w}{\partial y^2}+T_2\right]\left(1-\mu^2\nabla^2\right)M_{xy}\\ =\left(1-l^2\nabla^2\right)\left[B_{66}\left(\frac{\partial u}{\partial y}+\frac{\partial v}{\partial x}\right)-D_{66}\frac{\partial^2 w}{\partial x\partial y}\right].\end{aligned} \tag{2.8e}$$

In above relations, the details of coefficients

$$E_1=\int_{-\frac{h}{2}}^{\frac{h}{2}}E(z)dz=\left(E_m+\frac{E_c-E_m}{k+1}\right)h,\quad E_2=\int_{-\frac{h}{2}}^{\frac{h}{2}}zE(z)dz=\frac{(E_c-E_m)kh^2}{2(k+1)(k+2)}, \tag{2.9a}$$

$$E_3=\int_{-\frac{h}{2}}^{\frac{h}{2}}z^2E(z)dz=\left\{\frac{E_m}{12}+(E_c-E_m)\left[\frac{1}{k+3}-\frac{1}{k+2}+\frac{1}{4k+4}\right]\right\}h^3, \tag{2.9b}$$

and

$$A_{11}=A_{22}=\frac{E_1}{1-\nu^2},\quad A_{12}=A_{21}=\frac{\nu E_1}{1-\nu^2},\quad A_{33}=\frac{E_1}{2(1+\nu)}, \tag{2.10a}$$

$$B_{11}=B_{22}=\frac{E_2}{1-\nu^2},\quad B_{12}=B_{21}=\frac{\nu E_2}{1-\nu^2},\quad B_{33}=\frac{E_2}{1+\nu},\quad B_{66}=\frac{E_2}{2(1+\nu)}, \tag{2.10b}$$

$$D_{11}=D_{22}=\frac{E_3}{1-\nu^2},\quad D_{12}=D_{21}=\frac{\nu E_3}{1-\nu^2},\quad D_{66}=\frac{E_3}{1+\nu}. \tag{2.10c}$$

The general equilibrium equations of the FG cylindrical nanopanel resting on an elastic foundation can be obtained as [47,49,58]:

$$N_{x,x}+N_{xy,y}=0, \tag{2.11a}$$

$$N_{xy,x}+N_{y,y}=0, \tag{2.11b}$$

$$M_{x,xx}+2M_{xy,xy}+M_{y,yy}+\frac{1}{R}N_y+N_x w_{,xx}+2N_{xy}w_{,xy}+N_y w_{,yy}-q_f=0. \tag{2.11c}$$

3 Stability equations and Galerkin's method

In this section, the adjacent equilibrium criterion has been used to obtain the linearized stability equations of the FG cylindrical nanopanel resting on an elastic foundation. According to this criterion, the components of the displacement field at the new adjacent equilibrium configuration may be written as

$$u=u^0+u^1,\quad v=v^0+v^1,\quad w=w^0+w^1, \tag{3.1}$$

where (u_0,v_0,w_0) are components describer equilibrium position in the pre-buckling state and (u^1,v^1,w^1) are displacement components of a neighboring state of the stable equilibrium with respect to the equilibrium position.

Substituting the displacement components (3.1) into relations (2.7b), yields

$$N_x=N_x^0+N_x^1,\qquad N_\theta=N_\theta^0+N_\theta^1,\qquad N_{x\theta}=N_{x\theta}^0+N_{x\theta}^1, \tag{3.2a}$$

$$M_x=M_x^0+M_x^1,\qquad M_\theta=M_\theta^0+M_\theta^1,\qquad M_{x\theta}=M_{x\theta}^0+M_{x\theta}^1. \tag{3.2b}$$

Now, substituting Eqs. (3.1) and (3.2) into Eqs. (2.11a)-(2.11c) and note that the terms in the resulting equations with subscript 0 satisfy the equilibrium equations and therefore drop out of the equations, the stability equations for the FG cylindrical nanopanel resting on an elastic foundation can be represented as [57,58]

$$N^1_{x,x}+N^1_{xy,y}=0, \tag{3.3a}$$

$$N^1_{xy,x}+N^1_{y,y}=0, \tag{3.3b}$$

$$M^1_{x,xx}+2M^1_{xy,xy}+M^1_{y,yy}+\frac{1}{R}N^1_y+N^0_x w^1_{,xx}+2N^0_{xy}w^1_{,xy}+N^0_y w^1_{,yy}-q_f=0. \tag{3.3c}$$

In force resultants, superscript 1 refers to the state of stability, and superscript 0 refers to the state of equilibrium. The terms N_x^0, N_y^0 and N_{xy}^0 are the pre-buckling force resultants obtained from the linear equilibrium Eqs. (2.11a)-(2.11c).

Then, the system of stability equations of FG cylindrical nanopanel resting on an elastic foundation in the form of displacement components u^1, v^1 and w^1 according to the nonlocal strain gradient theory can be delivered by inserting the relation Eq. (2.8) into Eqs. (3.3a)-(3.3c) as follows:

$$\begin{aligned}&(1-l^2\nabla^2)\left[A_{11}\frac{\partial^2 u^1}{\partial x^2}+A_{12}\left(\frac{\partial^2 v^1}{\partial x\partial y}-\frac{1}{R}\frac{\partial w^1}{\partial x}\right)+A_{33}\left(\frac{\partial^2 u^1}{\partial y^2}+\frac{\partial^2 v^1}{\partial x\partial y}\right)\right.\\&\quad\left.-B_{11}\frac{\partial^3 w^1}{\partial x^3}-B_{12}\frac{\partial^3 w^1}{\partial x\partial y^2}-B_{33}\frac{\partial^3 w^1}{\partial x\partial y^2}\right]=0,\end{aligned}\tag{3.4a}$$

$$\begin{aligned}&(1-l^2\nabla^2)\left[A_{21}\frac{\partial^2 u^1}{\partial x\partial y}+A_{22}\left(\frac{\partial^2 v^1}{\partial y^2}-\frac{1}{R}\frac{\partial w^1}{\partial y}\right)+A_{33}\left(\frac{\partial^2 u^1}{\partial x\partial y}+\frac{\partial^2 v^1}{\partial x^2}\right)\right.\\&\quad\left.-B_{21}\frac{\partial^3 w^1}{\partial x^2\partial y}-B_{22}\frac{\partial^3 w^1}{\partial y^3}-B_{33}\frac{\partial^3 w^1}{\partial x^2\partial y}\right]=0,\end{aligned}\tag{3.4b}$$

$$\begin{aligned}&(1-l^2\nabla^2)\left[\frac{A_{21}}{R}\frac{\partial u^1}{\partial x}+\frac{A_{22}}{R}\left(\frac{\partial v^1}{\partial y}-\frac{w^1}{R}\right)+B_{11}\frac{\partial^3 u^1}{\partial x^3}+B_{12}\left(\frac{\partial^3 v^1}{\partial x^2\partial y}-\frac{1}{R}\frac{\partial^2 w^1}{\partial x^2}\right)\right.\\&\quad+B_{21}\left(\frac{\partial^3 u^1}{\partial x\partial y^2}-\frac{1}{R}\frac{\partial^2 w^1}{\partial x^2}\right)+B_{22}\left(\frac{\partial^3 v^1}{\partial y^3}-\frac{2}{R}\frac{\partial^2 w^1}{\partial y^2}\right)+2B_{66}\left(\frac{\partial^3 u^1}{\partial x\partial y^2}+\frac{\partial^3 v^1}{\partial x^2\partial y}\right)\\&\quad\left.-D_{11}\frac{\partial^4 w^1}{\partial x^4}-D_{12}\frac{\partial^4 w^1}{\partial x^2\partial y^2}-D_{21}\frac{\partial^4 w^1}{\partial x^2\partial y^2}-D_{22}\frac{\partial^4 w^1}{\partial y^4}-2D_{66}\frac{\partial^4 w^1}{\partial x^2\partial y^2}\right]\\&\quad+(1-\mu^2\nabla^2)\left(N_x^0\frac{\partial^2 w^1}{\partial x^2}+2N_{xy}^0\frac{\partial^2 w^1}{\partial x\partial y}+N_y^0\frac{\partial^2 w^1}{\partial y^2}\right)\\&\quad-(1-\mu^2\nabla^2)\left[K_1 w^1-K_2\left(\frac{\partial^2 w^1}{\partial x^2}+\frac{\partial^2 w^1}{\partial y^2}\right)\right]=0.\end{aligned}\tag{3.4c}$$

The Eqs. (3.4a)-(3.4c) are rewritten in a following form:

$$\begin{aligned}&A_{11}\left[\frac{\partial^2 u^1}{\partial x^2}-l^2\left(\frac{\partial^4 u^1}{\partial x^4}+\frac{\partial^4 u^1}{\partial y^2\partial x^2}\right)\right]+A_{12}\left[\frac{\partial^2 v^1}{\partial y\partial x}-l^2\left(\frac{\partial^4 v^1}{\partial y\partial x^3}+\frac{\partial^4 v^1}{\partial y^3\partial x}-\frac{1}{R}\frac{\partial^3 w^1}{\partial y^2\partial x}-\frac{1}{R}\frac{\partial^3 w^1}{\partial x^3}\right)\right.\\&\quad\left.-\frac{1}{R}\frac{\partial w^1}{\partial x}\right]+A_{33}\left[\frac{\partial^2 u^1}{\partial y^2}-l^2\left(\frac{\partial^4 u^1}{\partial y^2\partial x^2}+^2\frac{\partial^4 u^1}{\partial y^4}\right)-l^2\left(\frac{\partial^4 v^1}{\partial y\partial x^3}+\frac{\partial^4 v^1}{\partial y^3\partial x}\right)+\frac{\partial^2 v^1}{\partial y\partial x}\right]\\&\quad+B_{11}\left[l^2\left(\frac{\partial^5 w^1}{\partial y^2\partial x^3}+\frac{\partial^5 w^1}{\partial x^5}\right)-\frac{\partial^3 w^1}{\partial x^3}\right]+B_{12}\left[l^2\left(\frac{\partial^5 w^1}{\partial y^4\partial x}+\frac{\partial^5 w^1}{\partial y^2\partial x^3}\right)-\frac{\partial^3 w^1}{\partial y^2\partial x}\right]\\&\quad+B_{33}\left[l^2\left(\frac{\partial^5 w^1}{\partial y^4\partial x}+\frac{\partial^5 w^1}{\partial y^2\partial x^3}\right)-\frac{\partial^3 w^1}{\partial y^2\partial x}\right]=0,\end{aligned}\tag{3.5a}$$

$$A_{21}\left[\frac{\partial^2 u^1}{\partial y\partial x}-l^2\left(\frac{\partial^4 u^1}{\partial y\partial x^3}+\frac{\partial^4 u^1}{\partial y^3\partial x}\right)\right]+A_{22}\left\{\frac{1}{R}\left[l^2\left(\frac{\partial^3 w^1}{\partial y\partial x^2}+\frac{\partial^3 w^1}{\partial y^3}\right)-\frac{\partial w^1}{\partial y}\right]+\frac{\partial^2 v^1}{\partial y^2}\right.$$

$$-l^2\left(\frac{\partial^4 v^1}{\partial y^4}+\frac{\partial^4 v^1}{\partial y^2\partial x^2}\right)\Bigg\}+A_{33}\left[\frac{\partial^2 u^1}{\partial y\partial x}-l^2\left(\frac{\partial^4 u^1}{\partial y^3\partial x}+\frac{\partial^4 u^1}{\partial y\partial x^3}\right)+\frac{\partial^2 v^1}{\partial x^2}-l^2\left(\frac{\partial^4 v^1}{\partial x^4}+\frac{\partial^4 v^1}{\partial y^2\partial x^2}\right)\right]$$
$$+B_{21}\left[l^2\left(\frac{\partial^5 w^1}{\partial y^3\partial x^2}+\frac{\partial^5 w^1}{\partial y\partial x^4}\right)-\frac{\partial^3 w^1}{\partial y\partial x^2}\right]+B_{22}\left[l^2\left(\frac{\partial^5 w^1}{\partial y^3\partial x^2}+\frac{\partial^5 w^1}{\partial y^5}\right)-\frac{\partial^3 w^1}{\partial y^3}\right]$$
$$+B_{33}\left[l^2\left(\frac{\partial^5 w^1}{\partial y^3\partial x^2}+\frac{\partial^5 w^1}{\partial y\partial x^4}\right)-\frac{\partial^3 w^1}{\partial y\partial x^2}\right]=0, \tag{3.5b}$$

$$\frac{A_{21}}{R}\left[\frac{\partial u^1}{\partial x}-l^2\left(\frac{\partial^3 u^1}{\partial x^3}+\frac{\partial^3 u^1}{\partial y^2\partial x}\right)\right]+\frac{A_{22}}{R}\Bigg\{\frac{1}{R}\left[l^2\left(\frac{\partial^2 w^1}{\partial x^2}+\frac{\partial^2 w^1}{\partial y^2}\right)-w^1\right]+\frac{\partial v^1}{\partial y}$$
$$-l^2\left(\frac{\partial^3 v^1}{\partial y^3}+\frac{\partial^3 v^1}{\partial y\partial x^2}\right)\Bigg\}+B_{11}\left[\frac{\partial^3 u^1}{\partial x^3}-l^2\left(\frac{\partial^5 u^1}{\partial x^5}+\frac{\partial^5 u^1}{\partial y^2\partial x^3}\right)\right]$$
$$+B_{12}\Bigg\{\left[\frac{\partial^3 v^1}{\partial y\partial x^2}-l^2\left(\frac{\partial^5 v^1}{\partial y^3\partial x^2}+\frac{\partial^5 v^1}{\partial y\partial x^4}\right)\right]+\frac{1}{R}\left[l^2\left(\frac{\partial^4 w^1}{\partial y^2\partial x^2}+\frac{\partial^4 w^1}{\partial x^4}\right)-\frac{\partial^2 w^1}{\partial x^2}\right]\Bigg\}$$
$$+B_{21}\Bigg\{\frac{\partial^3 u^1}{\partial y^2\partial x}-l^2\left(\frac{\partial^5 u^1}{\partial y^2\partial x^3}+\frac{\partial^5 u^1}{\partial y^4\partial x}\right)+\frac{1}{R}\left[l^2\left(\frac{\partial^4 w^1}{\partial y^2\partial x^2}+\frac{\partial^4 w^1}{\partial x^4}\right)-\frac{\partial^2 w^1}{\partial x^2}\right]\Bigg\}$$
$$+D_{11}\left[l^2\left(\frac{\partial^6 w^1}{\partial x^6}+\frac{\partial^6 w^1}{\partial y^2\partial x^4}\right)-\frac{\partial^4 w^1}{\partial x^4}\right]+D_{12}\left[l^2\left(\frac{\partial^6 w^1}{\partial y^4\partial x^2}+\frac{\partial^6 w^1}{\partial y^2\partial x^4}\right)-\frac{\partial^4 w^1}{\partial y^2\partial x^2}\right]$$
$$+D_{21}\left[l^2\left(\frac{\partial^6 w^1}{\partial y^4\partial x^2}+\frac{\partial^6 w^1}{\partial y^2\partial x^4}\right)-\frac{\partial^4 w^1}{\partial y^2\partial x^2}\right]+B_{22}\Bigg\{\frac{2}{R}\left[l^2\left(\frac{\partial^4 w^1}{\partial y^2\partial x^2}+\frac{\partial^4 w^1}{\partial y^4}\right)-\frac{\partial^2 w^1}{\partial y^2}\right]$$
$$-l^2\left(\frac{\partial^5 v^1}{\partial y^3\partial x^2}+\frac{\partial^5 v^1}{\partial y^5}\right)+\frac{\partial^3 v^1}{\partial y^3}\Bigg\}+2B_{66}\left[\frac{\partial^3 u^1}{\partial y^2\partial x}+\frac{\partial^3 v^1}{\partial y\partial x^2}-l^2\left(\frac{\partial^5 u^1}{\partial y^2\partial x^3}+\frac{\partial^5 v^1}{\partial y\partial x^4}+\frac{\partial^5 v^1}{\partial y^3\partial x^2}+\frac{\partial^5 u^1}{\partial y^4\partial x}\right)\right]$$
$$+D_{22}\left[l^2\left(\frac{\partial^6 w^1}{\partial y^6}+\frac{\partial^6 w^1}{\partial y^4\partial x^2}\right)-\frac{\partial^4 w^1}{\partial y^4}\right]+2D_{66}\left[l^2\left(\frac{\partial^6 w^1}{\partial y^2\partial x^4}+\frac{\partial^6 w^1}{\partial y^4\partial x^2}\right)-\frac{\partial^4 w^1}{\partial y^2\partial x^2}\right]$$
$$+\left[1-\mu^2\left(\frac{\partial^2 w^1}{\partial x^2}+\frac{\partial^2 w^1}{\partial y^2}\right)\right]\left(N_x^0\frac{\partial^2 w^1}{\partial x^2}+2N_{xy}^0\frac{\partial^2 w^1}{\partial x\partial y}+N_y^0\frac{\partial^2 w^1}{\partial y^2}\right)$$
$$-\left[1-\mu^2\left(\frac{\partial^2 w^1}{\partial x^2}+\frac{\partial^2 w^1}{\partial y^2}\right)\right]\left[K_1 w^1-K_2\left(\frac{\partial^2 w^1}{\partial x^2}+\frac{\partial^2 w^1}{\partial y^2}\right)\right]=0. \tag{3.5c}$$

In this research, an analytical approach is used to study the buckling behavior of the FG cylindrical nanopanel resting on an elastic foundation under an axial compression load in the thermal environment. The FG cylindrical nanopanel is assumed to be simply supported on all edges and subjected to an axial compressive load, uniformly distributed along the curved edges of the nanopanel. Under the assumed loading, the pre-buckling force resultants are obtained as [57,58]

$$N_x^0=-\frac{P}{b}-T_1,\quad N_y^0=0,\quad N_{xy}^0=0. \tag{3.6}$$

The displacement and force boundary conditions for a simply supported FG cylindrical nanopanel are defined as [57,58]

$$w^1=0,\quad M_x^1=0,\quad N_x^1=N_x^0\qquad \text{at}\quad x=0,\quad x=L, \tag{3.7a}$$
$$w^1=0,\quad M_y^1=0,\quad N_y^1=N_y^0\qquad \text{at}\quad y=0,\quad y=b. \tag{3.7b}$$

The approximate solutions satisfying the boundary conditions (3.7) may be found in the forms [57,58]

$$u^1=U\cos\frac{m\pi x}{L}\sin\frac{n\pi y}{R\theta_0},\quad v^1=V\sin\frac{m\pi x}{L}\cos\frac{n\pi y}{R\theta_0},\quad w^1=W\sin\frac{m\pi x}{L}\sin\frac{n\pi y}{R\theta_0}, \tag{3.8}$$

where m and n are the number of half-waves in the generatrix direction, and the circumferential direction, respectively; and U, V, W are the amplitudes.

Substituting Eq. (3.8) into Eqs. (3.5a)-(3.5c), then applying Galerkin's method for the resulting equations. Finally, the resulting systems of equations are given as

$$X_{11}U+X_{12}V+X_{13}W=0, \tag{3.9a}$$

$$X_{21}U+X_{22}V+X_{23}W=0, \tag{3.9b}$$

$$X_{31}U+X_{32}V+(X_{33}+X_{34}N_x^0+X_{35}N_y^0+X_{36}K_1+X_{37}K_2)W=0, \tag{3.9c}$$

where the details of coefficients X_{ij} $(i=\overline{1,3};\ j=\overline{1,6})$ and η_k $(k=\overline{1,3})$ are defined in Appendix.

To derive the axial buckling force for the FG cylindrical nanopanel, the coefficient matrix of algebraic Eqs. (3.9a)-(3.9c) must be set equal to zero:

$$\begin{vmatrix} X_{11} & X_{12} & X_{13} \\ X_{21} & X_{22} & X_{23} \\ X_{31} & X_{32} & X_{33}+X_{34}N_x^0+X_{35}K_1+X_{36}K_2 \end{vmatrix}=0. \tag{3.10}$$

Developing this determinant and solving the resulting equation, the explicit expression to analyze the buckling of the FG cylindrical nanopanel subjected to an axial compressive load is delivered

$$X_{34}N_x^0=\frac{X_{31}(X_{12}X_{23}-X_{22}X_{13})-X_{32}(X_{11}X_{23}-X_{21}X_{13})}{(X_{21}X_{12}-X_{11}X_{22})}-X_{33}-X_{35}K_1-X_{36}K_2. \tag{3.11}$$

By noting expression of N_x^0 in Eq. (3.6), the critical axial buckling load (N_{cr}) is obtained by minimizing Eq. (3.10) with respect to m and n, the number of longitudinal and circumferential buckling waves.

4 Numerical results and discussion

4.1 Comparison studies

To verify the present work, two following comparisons are carried out.

First, compare the results obtained by the present study with the results achieved by Zhao and Liew [56] and Timosenko and Gere [59] for simply-supported isotropic cylindrical panel subjected to an axial compressive load is shown in Table 1. The panel dimensions are $L=10$in, span angle $\theta_0=0.2$rad, radius $R=50$in, and thickness $h=0.1$in. The

Table 1: Convergence of a simply-supported isotropic cylindrical panel under uniform compression ($h=0.1$in, $L=10$in, $\theta_0=0.2$rad, $R=50$in, $E=3.0\times10^6 psi$, $\nu=0.3$.).

	Zhao and Liew [56]				Timosenko and Gere [59]	present
	Mode					
	9×9	11×11	13×13	15×15		
$\overline{N_{cr}}=\frac{N_{cr}R}{Eh^2}$	0.6194	0.5963	0.5961	0.596	0.6052	0.575

Table 2: Convergence of a simply supported Al/ZrO2 panel under uniform compression ($h=0.001$m, $L=0.1$m, $R=0.5$m, $\theta=0.2$rad), error=(present-[56])*100/[56]. * Buckling mode (m,n).

	$\overline{N_{cr}}$						
	$k=0$	$k=0.5$	$k=1$	$k=2$	$k=5$	$k=10$	$k=20$
[56]	1.2768	1.039	0.9313	0.8366	0.7464	0.6933	0.6525
(mode)	1	1	1	1	1	1	1
Present	1.2404	1.0507	0.9584	0.8653	0.7571	0.6908	0.6424
(m,n)	(2,1)*	(2,1)	(2,1)	(2,1)	(2,1)	(2,1)	(2,1)
Error (%)	2.85	-1.13	-2.91	-3.43	-1.43	0.36	1.55

material properties are Young's modulus $E=3.0\times 106psi$ and Poisson ratio $v=0.3$. The critical buckling load for the isotropic cylindrical panel is defined as follows [56]:

$$\overline{N_{cr}}=\frac{N_{cr}R}{Eh^2}.$$

Second, the present study results and the ones obtained by Zhao and Liew [56] for the simply-supported FG cylindrical panel and the FG cylindrical panel subjected to an axial compressive load are compared in Table 2. The FG cylindrical panel is assumed to be made up of Aluminum (Al) and Zirconia (ZrO2). The Young's modulus of aluminum and Zirconia are $E_m=70$GPa and $E_c=151$GPa, respectively. The geometric properties of the panels are considered as: length $L=0.1$m, span angle $\theta_0=0.2$rad, radius $R=0.5$m, and thickness $h=0.001$m. The Poisson ratio is chosen as $\nu=10/3$. The critical buckling load for the FG cylindrical panel is defined as follows [56]:

$$\overline{N_{cr}}=\frac{N_{cr}R}{E_m h^2}.$$

Tables 1 and 2 indicated an excellent agreement between the obtained results of the present study and the results achieved by Zhao and Liew [56] and Timosenko and Gere [59].

4.2 Buckling analysis of FG cylindrical nanopanels

In this sub-section, the buckling response of the FG cylindrical nanopanel resting on an elastic foundation in a thermal environment based on the nonlocal strain gradient theory

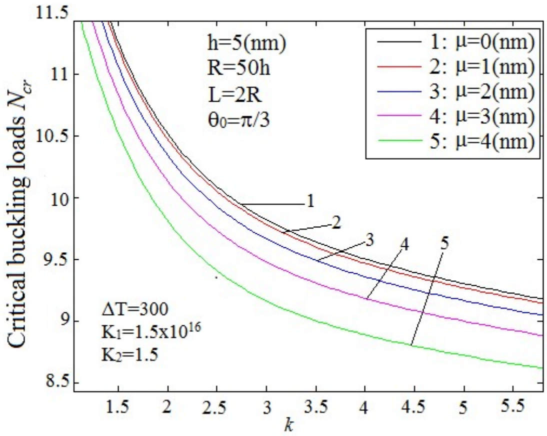

Figure 2: Effect of the volume fraction index (k) and the nonlocal parameter (μ) on the critical axial buckling load N_{cr}.

simple considering supported boundary conditions is explored. The material is Alumina-Aluminum FGM (Al2O3-Al), which has the following properties: $E_c=380$GPa, $\alpha_c=7\times 10^{-6}(^\circ C^{-1})$, $E_m=70$GPa, $\alpha_m=23\times 10^{-6}(^\circ C^{-1})$, and the Poisson's ratios $\nu_m=\nu_c=0.3$ [47]. The nonlocal parameter (μ) and material length scale parameter (l) vary from 0(nm) to 4(nm) [46,47,49].

Effects of the nonlocal parameter (μ), material length scale parameter (l), and the volume fraction index (k) on the critical buckling loads.

In Tables 3-5 and Figs. 2-4, the variations of critical buckling loads of the FG cylindrical nanopanel to the nonlocal parameter (μ) and the material length scale parameter (l) are illustrated for different values of the volume fraction index (k) and fixed values of $h=5$nm, $R=50h$, $L=2R$, $\theta_0=\frac{\pi}{3}$, $\Delta T=300$, $K_1=1.5\times 10^{16}$, $K_2=1.5$ [48]. For example, in Table 3 with the value of volume fraction index $k=2$ (and $l=0$), the critical buckling load decreases about 6.71% when the nonlocal parameter (μ) increases from 0 to 4; and in Table 4, with the value of volume fraction index $k=1$ (and $\mu=0$), the critical buckling load increases about 12.41% when the length scale parameter (l) increases from 0 to 4.

From these illustrations, it can be concluded that the critical buckling loads decrease (constant material length scale parameter) with the increasing of the nonlocal parameter (μ) due to stiffness-softening mechanism presented by nonlocal effects. However, stiffness-hardening mechanism due to strain gradients results in smaller critical buckling loads. So, the affections of nonlocality and strain gradient size-dependency on transient vibrations of nanopanel are opposite to each other. The above discussion reveals that both nonlocal and strain gradient parameters should be considered and accounted for modeling of nanostructures. Besides, it can be concluded from these illustrations, the critical buckling load does not change when $\mu=l$, which means that the obtained results of the nonlocal strain gradient theory are identical with the classical results if the material

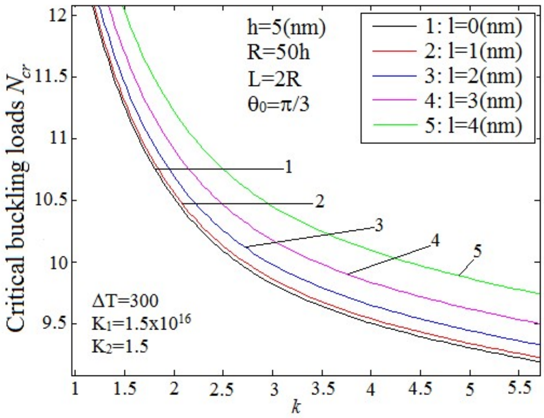

Figure 3: Effect of the volume fraction index (k) and the material length scale parameter (l) on the critical axial buckling load N_{cr}.

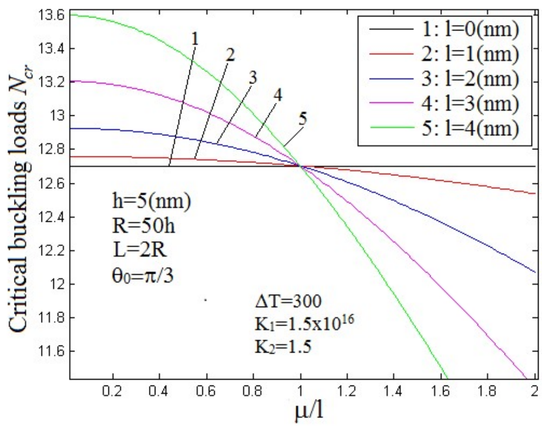

Figure 4: Effect of the nonlocal parameter μ and the material length scale parameter l on the critical buckling loads.

length scale parameter is equal to the nonlocal parameter ($\mu = l$). These illustrations also indicate that at a fixed nonlocal parameter (μ) and/ or the material length scale parameter (l), an increment in the volume fraction index (k) leads to a decreasing of the buckling load. This is due to the reason that by increasing the value of the volume fraction index (k), the percentage of metal phase will rise, thus makes the FG cylindrical nanopanel less rigid.

Moreover, it can be seen from Table 5 and Fig. 4 that the results at $\mu/l = 0$ and $l = 0$ illustrate those of the nonlocal elasticity theory. When $\mu/l = 1$, the nonlocal strain gradient theory results are identical with the classical results. It is of interest that when $\mu > l$, at a certain scale ratio (μ/l), the critical buckling loads decrease as the material length

Table 3: Effect of the volume fraction index (k) and the nonlocal parameter (μ) on the critical axial buckling load N_{cr} ($h=5$nm, $R=50$h, $L=2R$, $\theta_0=\frac{\pi}{3}$, $\Delta T=300$, $K_1=1.5\times10^{16}$, $K_2=1.5$). * Buckling mode (m,n).

N_{cr}	k					
μ (nm)	0	0.5	1	2	5	10
0	24.0155	15.8427	12.7028	10.5222	9.3096	8.705
	(9,1)*	(9,1)	(10,1)	(10,1)	(10,1)	(10,1)
1	23.9374	15.7884	12.6469	10.4782	9.2746	8.6746
	(9,1)	(9,1)	(10,1)	(10,1)	(10,1)	(10,1)
2	23.7061	15.5933	12.4822	10.3485	9.1713	8.5848
	(9,1)	(10,1)	(10,1)	(10,1)	(10,1)	(10,1)
3	23.3306	15.2587	12.2163	10.1391	9.0046	8.4383
	(9,1)	(10,1)	(10,1)	(10,1)	(10,1)	(11,1)
4	22.8249	14.8117	11.8612	9.8166	8.7269	8.187
	(9,1)	(10,1)	(10,1)	(10,1)	(11,1)	(11,1)

Table 4: Effect of the volume fraction index (k) and the material length scale parameter (l) on the critical axial buckling load N_{cr} ($h=5$nm, $R=50h$, $L=2R$, $\theta_0=\frac{\pi}{3}$, $\Delta T=300$, $K_1=1.5\times10^{16}$, $K_2=1.5$). * Buckling mode (m,n).

N_{cr}	k					
l (nm)	0	0.5	1	2	5	10
0	24.0155	15.8427	12.7028	10.5222	9.3096	8.705
	(9,1)	(9,1)	(10,1)	(10,1)	(10,1)	(10,1)
1	24.0939	15.8972	12.7588	10.5663	9.3447	8.7356
	(9,1)	(9,1)	(10,1)	(10,1)	(10,1)	(10,1)
2	24.329	16.0607	12.9269	10.6987	9.4501	8.8272
	(9,1)	(9,1)	(10,1)	(10,1)	(10,1)	(10,1)
3	25.2697	16.3331	13.2071	10.9193	9.6258	8.9799
	(9,1)	(9,1)	(10,1)	(10,1)	(10,1)	(10,1)
4	25.2697	16.7146	14.2786	11.2283	9.8717	9.1938
	(9,1)	(9,1)	(10,1)	(10,1)	(10,1)	(10,1)

scale parameter l increases. However, when $\mu<l$, the critical buckling loads increase at a certain scale ratio (μ/l) as the material length scale parameter l increases. These phenomena show that the FG cylindrical nanopanel exerts a stiffness-softening effect when $\mu>l$ and exerts a stiffness-hardening effect when $\mu<l$.

Effect of R/h and L/R ratios on the critical buckling loads.

Figs. 5-8 illustrate the effects of R/h and L/R ratios on the critical buckling loads N_{cr} of the FG cylindrical nanopanel resting on elastic foundation in a thermal environment when R is constant. It is indicated that the critical buckling loads N_{cr} decrease strongly when the R/h ratio increases. This is obvious because of increasing ratio R/h, h will be reduced, and thus the FG cylindrical nanopanel becomes softer. In addition, it is easily seen that the L/R ratio has no apparent effect on the critical axial buckling load N_{cr} when

Table 5: Effect of the volume fraction index (k) and the material length scale parameter (l) on the critical axial buckling load N_{cr} ($h=5$nm, $R=50h$, $L=2R$, $\theta_0=\frac{\pi}{3}$, $\Delta T=300$, $K_1=1.5\times10^{16}$, $K_2=1.5$). * Buckling mode (m,n).

N_{cr}	l (nm)				
μ (nm)	0	1	2	3	4
0	12.7028	12.7588	12.9269	13.2071	14.2786
	(10,1)*	(10,1)	(10,1)	(10,1)	(10,1)
1	12.6469	12.7028	12.8702	13.1492	13.5399
	(10,1)	(10,1)	(10,1)	(10,1)	(10,1)
2	12.4822	12.5373	12.7028	12.9784	13.3644
	(10,1)	(10,1)	(10,1)	(10,1)	(10,1)
3	12.2163	12.2704	12.4325	12.7028	13.0811
	(10,1)	(10,1)	(10,1)	(10,1)	(10,1)
4	11.8612	11.9138	12.0716	12.3346	12.7028
	(10,1)	(10,1)	(10,1)	(10,1)	(10,1)

the L/R ratio increases. From Figs. 7 and 8 with the ratio L/R is small $(L/R<2)$, the critical buckling loads N_{cr} of the FG cylindrical nanopanel varies quite complicatedly to the ratio L/R; on the other hand, with larger values of the ratio L/R, the ratio L/R has a little effect on the critical buckling loads N_{cr} of the FG cylindrical nanopanel. Generally, the critical axial load N_{cr} decreases as an increase in the L/R ratio.

Effect of span angle θ_0 on the critical buckling loads.

Figs. 9 and 10, respectively, show the effect of span angle θ_0 on the critical axial buckling loads N_{cr} of the FG cylindrical nanopanel resting on elastic foundation in the thermal environment with different values of the nonlocal parameter (μ) and material length scale parameter (l). It can be seen that, for small values of the span angle ($\theta_0 \le 1rad \approx 60°$), the

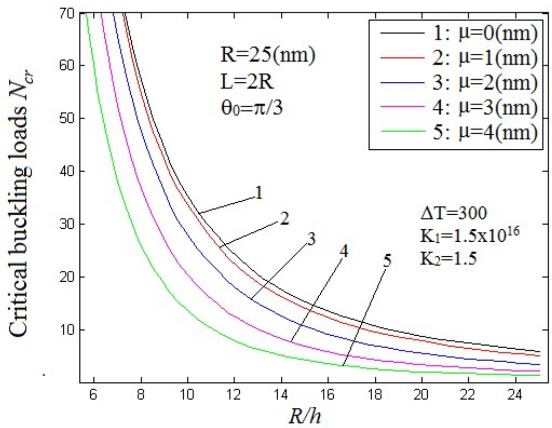

Figure 5: Effect of R/h on the critical axial buckling load N_{cr}.

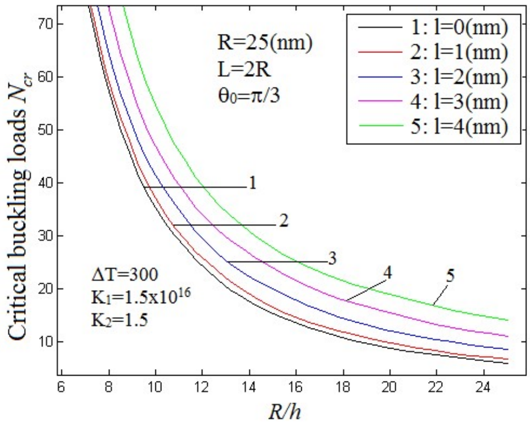

Figure 6: Effect of R/h on the critical bucklingload N_{cr}.

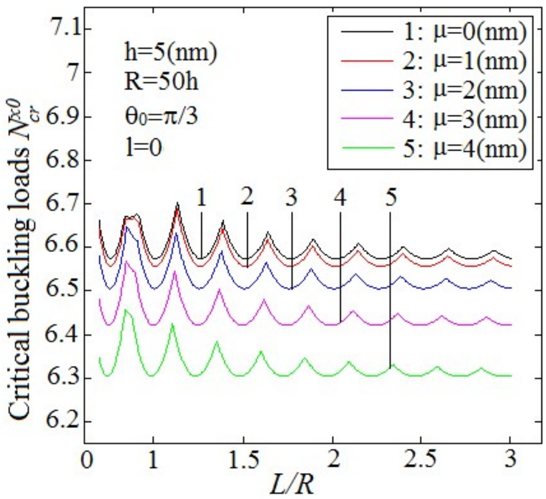

Figure 7: Effect of L/R ratio on the critical buckling load N_{cr} for some values of the nonlocal parameter μ.

critical axial buckling load N_{cr} decreases rapidly when the span angle θ_0 increases; however, for higher values of the span angle, the critical axial load N_{cr} does not change much when the span angle changes.

Effect of the thermal environment on the critical axial buckling load N_{cr}.

Tables 6 and 7 examine the effect of the thermal environment on the critical axial buckling load N_{cr} of the FG cylindrical nanopanel resting on an elastic foundation with respect to the nonlocal parameter (μ) and the material length scale parameter (l). It can be seen that an increase in the temperature level of the FG cylindrical nanopanel leads to a significant decrease in the critical axial buckling load of the nanopanel. For example, with

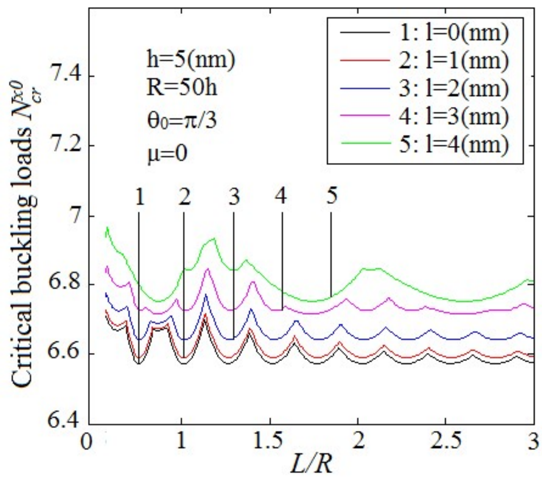

Figure 8: Effect of L/R ratio on the critical buckling load N_{cr} for some values of the material length scale parameter l.

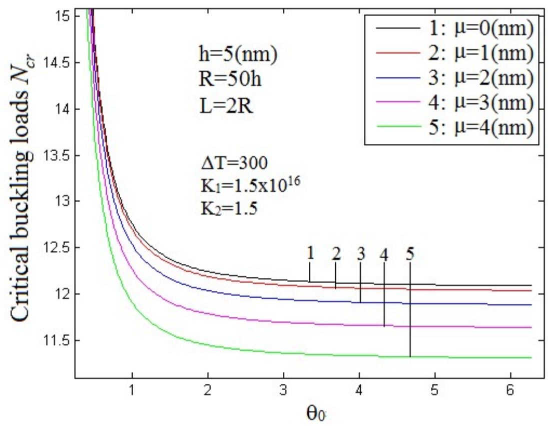

Figure 9: Effect of span angle θ_0 on the critical axial buckling load N_{cr} for some values of the nonlocal parameter μ.

$\Delta T = 500$K is presented in Table 6, as the nonlocal parameter $\mu = (0,1,2,3,4)$, the critical axial buckling loads of FG cylindrical nanopanel resting on an elastic foundation decrease from 55.53% to 58.09%; and with $\Delta T = 500$K is presented in Table 7, as the material length scale parameter $l = (0,1,2,3,4)$, the critical axial buckling loads FG cylindrical nanopanel decrease from 55.53% to 53.03%. This is expected due to the reduction in material stiffness as the temperature elevates.

Effect of elastic foundation on the critical axial buckling load N_{cr}.

Variations of the critical axial buckling load of the FG cylindrical nanopanel in the thermal environment with or without a Winkler–Pasternak type elastic foundation are

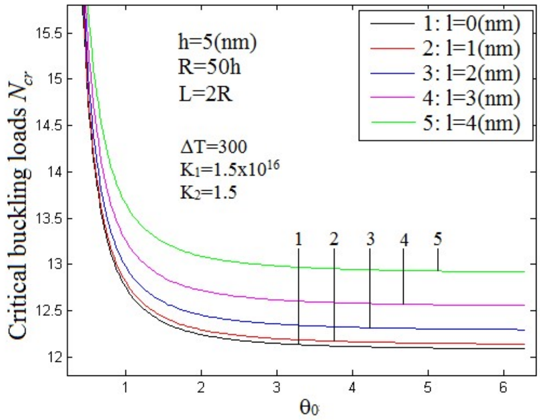

Figure 10: Effect of span angle θ_0 on the critical axial buckling load N_{cr} for some values of the material length scale parameter l.

presented in Table 8. According to this table, by increasing the Winkler/ shear modulus parameters, the critical axial buckling load of the FG cylindrical nanopanel increase. It is entirely appropriate because the elastic foundation increases the stiffness of the FG cylindrical nanopanel. For example, comparing the values of critical axial buckling loads of the FG cylindrical nanopanel with or without the elastic foundations, for $K_2=0$ and $K_1=1\times10^{16}$; 1.3×10^{16}, 1.5×10^{16}, 1.8×10^{16}; 2×10^{16} [39], the effect on N_{cr} are 49.6%, 61.73%, 69.75%, 81.79%, 89.82%, respectively; corresponding to values of K_1 from 1×10^{16} to 2×10^{16}, the critical axial buckling loads increase from 7.96% to 9.88% when increasing values of K_2 from 0 to 2. The critical axial buckling load $N_{cr}=14.0551$ ($K_1=2\times10^{16}$, $K_2=2$) increases by about 122.65% compared to $N_{cr}=6.3125$ ($K_1=0$, $K_2=0$).

Table 6: Effect of the thermal environment on critical axial buckling load N_{cr} with respect to nonlocal parameter ($h=5$nm, $R=50h$, $L=2R$, $\theta_0=pi/3$, $k=1$, $K_1=1.5\times10^{16}$, $K_2=1.5$). * Buckling mode (m,n).

N_{cr}	$\Delta T(K)$						
μ (nm)	-100	-50	0	100	200	300	500
0	21.1647 (10,1)	20.1069 (10,1)	19.0492 (10,1)	16.9337 (10,1)	14.8182 (10,1)	12.7028 (10,1)	8.4718 (10,1)
1	21.1088 (10,1)	20.0511 (10,1)	18.9934 (10,1)	16.8779 (10,1)	14.7624 (10,1)	12.6469 (10,1)	8.416 (10,1)
2	20.9441 (10,1)	19.8864 (10,1)	18.8286 (10,1)	16.7132 (10,1)	14.5977 (10,1)	12.4822 (10,1)	8.2513 (10,1)
3	20.6782 (10,1)	19.6205 (10,1)	18.5628 (10,1)	16.4473 (10,1)	14.3318 (10,1)	12.2163 (10,1)	7.9854 (10,1)
4	20.3231 (10,1)	19.2654 (10,1)	18.2077 (10,1)	16.0922 (10,1)	13.9767 (10,1)	11.8612 (10,1)	7.6303 (10,1)

Table 7: Effect of the thermal environment on critical axial buckling load N_{cr} with respect to material length scale parameter ($h=5$nm, $R=50h$, $L=2R$, $\theta_0=pi/3$, $k=1$, $K_1=1.5\times10^{16}$, $K_2=1.5$). * Buckling mode (m,n).

N_{cr}	$\Delta T(K)$						
l (nm)	-100	-50	0	100	200	300	500
0	21.1647	20.1069	19.0492	16.9337	14.8182	12.7028	8.4718
	(10,1)	(10,1)	(10,1)	(10,1)	(10,1)	(10,1)	(10,1)
1	21.2207	20.1630	19.1052	16.9897	14.8743	12.7588	8.5278
	(10,1)	(10,1)	(10,1)	(10,1)	(10,1)	(10,1)	(10,1)
2	21.3888	20.3311	19.2733	17.1579	15.0424	12.9269	8.6959
	(10,1)	(10,1)	(10,1)	(10,1)	(10,1)	(10,1)	(10,1)
3	21.6690	20.6113	19.5535	17.438	15.3226	13.2071	8.9761
	(10,1)	(10,1)	(10,1)	(10,1)	(10,1)	(10,1)	(10,1)
4	22.0613	21.0035	19.9458	17.8303	15.7148	13.5993	9.3684
	(10,1)	(10,1)	(10,1)	(10,1)	(10,1)	(10,1)	(10,1)

Table 8: Effect of elastic foundation on critical axial buckling load N_{cr} ($h=5$nm, $R=50h$, $L=2R$, $\theta_0=pi/3$, $k=1$, $\Delta T=300$, $\mu=3$, $l=1$), $error=[N_{cr}(K_2=2)-N_{cr}(K_2=0)]*100/N_{cr}\ (K_2=0)$. * Buckling mode (m,n).

N_{cr} k_2	K_1					
	0	1×10^{16}	1.3×10^{16}	1.5×10^{16}	1.8×10^{16}	2×10^{16}
0	6.3125	9.4491	10.2091	10.7157	11.4756	11.9822
	(8,1)*	(10,1)	(10,1)	(10,1)	(10,1)	(10,1)
1	-	10.4856	11.2455	11.7521	12.512	13.0187
		(10,1)	(10,1)	(10,1)	(10,1)	(10,1)
1.3	-	10.7966	11.5565	12.0631	12.823	13.3296
		(10,1)	(10,1)	(10,1)	(10,1)	(10,1)
1.5	-	11.0039	11.7638	12.2704	13.0303	13.5369
		(10,1)	(10,1)	(10,1)	(10,1)	(10,1)
2	-	11.5221	12.282	12.7886	13.5485	14.0551
		(10,1)	(10,1)	(10,1)	(10,1)	(10,1)
error		9.88	9.22	8.82	8.28	7.96

5 Conclusions

In this study, an analytical approach is utilized to analyze the mechanical buckling of the FG cylindrical nanopanel resting on an elastic foundation in the thermal environment by using the nonlocal strain gradient theory. The material properties of nanopanel are varied by power-law distribution along with the thickness. The equilibrium equations are derived via the adjacent equilibrium criterion. The analytical solution for buckling analysis of the supported cylindrical nanopanel under the axial compressive load and the thermal environment is performed using Galerkin's solution. The comparison shows that the present results are in good agreement with the published results in the literature. The numerical results support the following conclusions:

i) The value of critical axial buckling loads of the FG cylindrical nanopanel resting on an elastic foundation in the thermal environment decreases when the nonlocal parameter (μ) increases; and vice versa, the value of critical buckling loads of the FG cylindrical nanopanel increases when the material length scale parameter (l) increases. Furthermore, the FG cylindrical nanopanel exerts a stiffness-softening effect when $\mu > l$ and exerts a stiffness-hardening effect when $\mu < l$.

ii) The critical axial buckling load (N_{cr}) decreases strongly when increasing the R/h ratio and volume fraction index k.

iii) The critical axial buckling load (N_{cr}) generally decreases when the L/R ratio and span angle θ_0 increases.

iv) The temperature has had a significant effect on the critical axial buckling load (N_{cr}) of the FG cylindrical nanopanel resting on an elastic foundation. The critical axial buckling load (N_{cr}) decreases with an increase in temperature.

v) The critical axial buckling load (N_{cr}) of the FG cylindrical nanopanel resting on an elastic foundation in the thermal environment increases gradually with increasing the coefficients of elastic foundation.

Appendix

$$
\begin{aligned}
X_{11} &= -\frac{\pi^2\left[R^2\theta_0^2\left(L^2+\pi^2l^2m^2\right)+n^2\pi^2l^2L^2\right]}{4L^3R^3\theta_0^3}\left(m^2R^2\theta_0^2A_{11}+n^2L^2A_{33}\right),\\
X_{12} &= -\frac{n\pi^2m\left[R^2\theta_0^2\left(L^2+\pi^2l^2m^2\right)+n^2\pi^2l^2L^2\right]}{4R^2\theta_0^2L^2}\left(A_{12}+A_{33}\right),\\
X_{13} &= \frac{\pi m\left[R^2\theta_0^2\left(L^2+\pi^2l^2m^2\right)+n^2\pi^2l^2L^2\right]}{4L^4R^3\theta_0^3}\left[\left(\pi^2m^2RB_{11}-L^2A_{12}\right)R\theta_0^2+n^2\pi^2L^2\left(B_{12}+B_{33}\right)\right],\\
X_{21} &= -\frac{n\pi^2m\left[\left(\pi^2l^2m^2+L^2\right)R^2\theta_0^2+n^2\pi^2l^2L^2\right]}{4L^2R^2\theta_0^2}\left(A_{21}+A_{33}\right),\\
X_{22} &= -\frac{\pi^2\left[\left(\pi^2l^2m^2+L^2\right)R^2\theta_0^2+n^2\pi^2l^2L^2\right]}{4L^3R^3\theta_0^3}\left(n^2L^2A_{22}+m^2R^2\theta_0^2A_{33}\right),\\
X_{23} &= \frac{n\pi\left[\left(\pi^2l^2m^2+L^2\right)R^2\theta_0^2+n^2\pi^2l^2L^2\right]}{4L^3R^4\theta_0^4}\left[L^2\left(n^2\pi^2B_{22}-R\theta_0^2A_{22}\right)+\pi^2m^2R^2\theta_0^2\left(B_{21}+B_{33}\right)\right],\\
X_{31} &= \frac{\pi m\left[\left(L^2+\pi^2l^2m^2\right)\theta_0^2R^2+n^2\pi^2l^2L^2\right]}{4L^4R^3\theta_0^3}\left[\left(m^2R\pi^2B_{11}-L^2A_{21}\right)R\theta_0^2+L^2\pi^2n^2\left(B_{21}+2B_{66}\right)\right],
\end{aligned}
$$

$$X_{32}=\frac{n\pi\left(\left(L^2+\pi^2l^2m^2\right)\theta_0^2R^2+n^2\pi^2l^2L^2\right)}{4L^3R^4\theta_0^4}\left[L^2\left(n^2\pi^2B_{22}-R\theta_0^2A_{22}\right)+\pi^2m^2R^2\theta_0^2\left(B_{12}+2B_{66}\right)\right],$$

$$X_{33}=-\frac{\left[\left(L^2+\pi^2l^2m^2\right)\theta_0^2R^2+n^2\pi^2l^2L^2\right]}{4L^5R^5\theta_0^5}\Big[L^4R^2\theta_0^4A_{22}+n^2\pi^2L^4\left(n^2\pi^2D_{22}-2R\theta_0^2B_{22}\right)$$
$$-\pi^2L^2\theta_0^4m^2R^3\left(B_{12}+B_{21}\right)+m^4R^4\theta_0^4\pi^4D_{11}+L^2\theta_0^2m^2n^2R^2\pi^4\left(D_{12}+D_{21}+2D_{66}\right)\Big],$$

$$X_{34}=\frac{h\pi^2m^2\left[\mu^2\pi^2n^2L^2+\left(\mu^2\pi^2m^2+L^2\right)R^2\theta_0^2\right]}{4RL^3\theta_0},$$

$$X_{35}=\frac{h\pi^2n^2\left[\mu^2\pi^2n^2L^2+\left(\mu^2\pi^2m^2+L^2\right)R^2\theta_0^2\right]}{4R^3L\theta_0^3},$$

$$X_{36}=\frac{R^2L^2\theta_0^2+\mu^2\pi^2m^2R^2\theta_0^2+\mu^2\pi^2n^2L^2}{4RL\theta_0},$$

$$X_{37}=\frac{\pi^2\left(R^2\theta_0^2m^2+n^2L^2\right)\left(R^2L^2\theta_0^2+\mu^2\pi^2m^2R^2\theta_0^2+\mu^2\pi^2n^2L^2\right)}{4R^3L^3\theta_0^3}.$$

Acknowledgements

The authors would like to thank the reviewers for their valuable comments and suggestions to improve the clarity of this study. This research is funded by the Vietnam National Foundation for Science and Technology Development (NAFOSTED) under grant number 107.02–2020.03. The authors are grateful for this support.

References

[1] P. CHAUHAN, AND I. KHAN, *Review on analysis of functionally graded material beam type structure,* Int. J. Adv. Mech. Eng., 4(3) (2014), pp. 299–306.

[2] A. HASSAN, AND N. KURGAN, *A review on buckling analysis of functionally graded plates under thermo-mechanical loads,* Int. J. Eng. Appl. Sci., 11(1) (2019), pp. 345–368.

[3] H. DAI, Y. RAO, AND T. DAI, *A review of recent researches on FGM cylindrical structures under coupled physical interactions,* Compos. Struct., 152 (2016), pp. 199–225.

[4] M. NEJAD, M. JABBARI, AND A. HADI, *A review of functionally graded thick cylindrical and conical shells,* J. Comput. Appl. Mech., 48(2) (2017), pp. 357–370.

[5] A. ERIGEN, AND D. EDELEN, *On nonlocal elasticity,* Int. J. Eng. Sci., 10 (1972), pp. 233–248.

[6] A. ERIGEN, *On differential equations of nonlocal elasticity and solutions of screw dislocation and surface waves,* J. Appl. Phys., 54 (1983), 4703.

[7] M. GURTIN, AND A. MURDOCH, *A continuum theory of elastic material surfaces,* Arch. Rat. Mech. Anal., 57(4) (1975), pp. 290–323.

[8] M. GURTIN, AND A. MURDOCH, *Surface stress in solids,* Int. J. Solids. Struct., 14(6) (1978), pp. 431–440.

[9] R. ANSARI, AND S. SAHMANI, *Surface stress effects on the free vibration behavior of nanoplates,* Int. J. Eng. Sci., 49 (2011), pp. 1204–1215.

[10] W. Nowacki, *Couple-stresses in the theory of thermoelasticity,* in: H. Parkus and L. Sedov (eds), Irreversible Aspects of Continuum Mechanics and Transfer of Physical Characteristics in Moving Fluids, IUTAM Symposia, 1968, pp. 259–278.

[11] R. Toupin, *Theories of elasticity with couple-stress,* Arch. Rat. Mech. Anal., 17 (1964), pp. 85–112.

[12] F. Yang, A. Chong, D. Lam, and P. Tong, *Couple stress based strain gradient theory for elasticity,* Int. J. Solids. Struct., 39 (2002), pp. 2731–2743.

[13] A. Hadjesfandiari, and G. Dargush, *Couple stress theory for solids,* Int. J. Solids. Struct., 48 (2011), pp. 2496–2510.

[14] M. Shaat, F. Mahmoud, X. Gao, and A. Faheem, *Size-dependent bending analysis of Kirchhoff nano-plates based on a modified couple-stress theory including surface effects,* Int. J. Mech. Sci., 79 (2014), pp. 31–37.

[15] M. Eltaher, A. Abdelrahman, and I. Esen, *Dynamic analysis of nanoscale Timoshenko CNTs based on doublet mechanics under moving load,* Euro. Phys. J. Plus, 136(7) (2021), pp. 1–21.

[16] M. Eltaher, and N. Mohamed, *Nonlinear stability and vibration of imperfect CNTs by Doublet mechanics,* Appl. Math. Comput., 382 (2020), 125311.

[17] M. Eltaher, N. Mohamed, and S. Mohamed, *Nonlinear buckling and free vibration of curved CNTs by doublet mechanics,* Smart. Struct. Syst., 26(2) (2020), pp. 213–226.

[18] N. Mohamed, S. Mohamed, and M. Eltaher, *Buckling and post-buckling behaviors of higher order carbon nanotubes using energy-equivalent model,* Eng. Comput., 37 (2021), pp. 2823–2836.

[19] N. Mohamed, M. Eltaher, S. Mohamed, and L. Seddek, *Energy equivalent model in analysis of postbuckling of imperfect carbon nanotubes resting on nonlinear elastic foundation,* Struct. Eng. Mech., 70(6) (2019), pp. 737–750.

[20] M. Eltaher, N. Mohamed, S. Mohamed, and L. Seddek, *Postbuckling of curved carbon nanotubes using energy equivalent model,* J. Nano. Res., 57 (2019), pp. 136–157.

[21] C. Lim, G. Zhang, and J. Reddy, *A higher-order nonlocal elasticity and strain gradient theory and its applications in wave propagation,* J. Mech. Phys. Solids, 78 (2015), pp. 298–313.

[22] M. Ghadiri, N. Shafei, and H. Safarpour, *Influence of surface effects on vibration behavior of a rotary functionally graded nanobeam based on Eringen's nonlocal elasticity,* Microsystem. Tech., 23 (2017), pp. 1045–1065.

[23] M. Şimşek, *Nonlinear free vibration of a functionally graded nanobeam using nonlocal strain gradient theory and a novel Hamiltonian approach,* Int. J. Eng. Sci., 105 (2016), pp. 12–27.

[24] F. Mehralian, and Y. Beni, *A nonlocal strain gradient shell model for free vibration analysis of functionally graded shear deformable nanotubes,* Int. J. Eng. Appl. Sci., 9(2) (2017), pp. 88–102.

[25] A. Abdelrahman, I. Esen, R. Shaltout, M. Eltaher, and A. Assie, *Dynamics of perforated higher order nanobeams subject to moving load using the nonlocal strain gradient theory,* Smart. Struct. Syst., 28(4) (2021), pp. 515–533.

[26] I. Esen, A. Abdelrahman, and M. Eltaher, *On vibration of sigmoid/symmetric functionally graded nonlocal strain gradient nanobeams under moving load,* Int. J. Mech. Mater. Des., 17(3) (2021), pp. 721–742.

[27] D. Chen, J. Yang, and S. Kitipornchai, *Nonlinear vibration and postbuckling of functionally graded graphene reinforced porous nanocomposite beams,* Compos. Sci. Tech., 142 (2017), pp. 235–245.

[28] M. Attia, *On the mechanics of functionally graded nanobeams with the account of surface elasticity,* Int. J. Eng. Sci., 115 (2017), pp. 73–101.

[29] M. AREFI, AND A. SOLTAN ARANI, *Higher order shear deformation bending results of a magneto-electro-thermo-elastic functionally graded nanobeam in thermal, mechanical, electrical, and magnetic environments,* Mech. Based Des. Struct. Mach., 46(6) (2018), pp. 669–692.

[30] M. AREFI, AND A. ZENKOUR, *A simplified shear and normal deformations nonlocal theory for bending of functionally graded piezomagnetic sandwich nanobeams in magneto-thermo-electric environment,* J. Sandw. Struct. Mater., 18(5) (2016), pp. 624–651.

[31] M. AREFI, AND A. ZENKOUR, *Wave propagation analysis of a functionally graded magneto-electroelastic nanobeam rest on visco-Pasternak foundation,* Mech. Res. Commun., 79 (2017), pp. 51–62.

[32] M. BARATI, AND A. ZENKOUR, *Post-buckling analysis of imperfect multi-phase nanocrystalline nanobeams considering nanograins and nanopores surface effects,* Compos. Struct., 184 (2018), pp. 497–505.

[33] M. BARATI, AND A. ZENKOUR, *Thermal post-buckling analysis of closed circuit flexoelectric nanobeams with surface effects and geometrical imperfection,* Mech. Adv. Mater. Struct., 26(17) (2018), pp. 1482–1490.

[34] F. EBRAHIMI, AND E. SALARI, *Effect of various thermal loadings on buckling and vibrational characteristics of nonlocal temperature-dependent functionally graded nanobeams,* Mech. Adv. Mater. Struct., 23(12) (2016), pp. 1379–1397.

[35] F. EBRAHIMI, AND M. BARATI, *Vibration analysis of nonlocal beams made of functionally graded material in thermal environment,* Euro. Phys. J. Plus, 131 (2016), 279.

[36] F. EBRAHIMI, AND M. BARATI, *A modified nonlocal couple stress based beam model for vibration analysis of higher-order FG nanobeams,* Mech. Adv. Mater. Struct., 25(13) (2018), pp. 1121–1132.

[37] F. EBRAHIMI, AND M. BARATI, *A nonlocal strain gradient refined beam model for buckling analysis of size-dependent shear-deformable curved FG nanobeams,* Compos. Struct., 159 (2017), pp. 174–182.

[38] A. ZENKOUR, AND M. AREFI, *Nonlocal transient electro-thermo-mechanical vibration and bending analysis of a functionally graded piezoelectric single-layered nanosheet rest on visco-Pasternak foundation,* J. Therm. Stress., 40 (2017), pp. 167–184.

[39] R. ANSARI, M. FAGHIH SHOJAEI, V. MOHAMMADI, R. GHOLAMI, AND M. DARABI, *Nonlinear vibrations of functionally graded Mindlin microplates based on the modified couple stress theory,* Compos. Struct., 114 (2014), pp. 124–134.

[40] R. KOLAHCHI, M. BIDGOLI, G. BEYGIPOOR, AND M. FAKHAR, *A nonlocal nonlinear analysis for buckling in embedded FG-SWCNT-reinforced microplates subjected to magnetic field,* J. Mech. Sci. Tech., 29(9) (2015), pp. 3669–3677.

[41] A. ASHOORI, E. SALARI, AND S. SADOUGH VANINI, *Size-dependent thermal stability analysis of embedded functionally graded annular nanoplates based on the nonlocal elasticity theory,* Int. J. Mech. Sci., 119 (2016), pp. 396–411.

[42] A. DAIKH, M. HOUARI, AND M. ELTAHER, *A novel nonlocal strain gradient Quasi-3D bending analysis of sigmoid functionally graded sandwich nanoplates,* Compos. Struct., 262 (2021), 113347.

[43] F. EBRAHIMI, AND E. HEIDARI, *Surface effects on nonlinear vibration of embedded functionally graded nanoplates via higher order shear deformation plate theory,* Mech. Adv. Mater. Struct., 26(8) (2019), pp. 671–699.

[44] Z. SHARIFI, R. KHORDAD, A. GHARAATI, AND G. FOROZANI, *An analytical study of vibration in functionally graded piezoelectric nanoplates: nonlocal strain gradient theory,* Appl. Math. Mech., 2019. 40(12) (2019), pp. 1723–1740.

[45] M. BARATI, AND H. SHAHVERDI, *Hygro-thermal vibration analysis of graded double-refined-nanoplate systems using hybrid nonlocal stress-strain gradient theory,* Compos. Struct., 176

(2017), pp. 982–995.

[46] M. ABAZID, *The Nonlocal Strain Gradient Theory for Hygrothermo-Electromagnetic Effects on Buckling, Vibration and Wave Propagation in Piezo-electro-magnetic Nanoplates,* Int. J. Appl. Mech., 11(7) (2019), 1950067.

[47] M. BARATI, *Vibration analysis of porous FG nanoshells with even and uneven porosity distributions using nonlocal strain gradient elasticity,* Acta. Mech., 229 (2018), pp. 1183–1196.

[48] M. AREFI, E. BIDGOLI, AND O. CIVALEK, *Bending response of FG composite doubly curved nanoshells with thickness stretching via higher-order sinusoidal shear theory,* Mech. Based. Des. Struct. Mach., (2020).

[49] S. SAHMANI, AND M. AGHDAM, *Size dependency in axial postbuckling behavior of hybrid FGM exponential shear deformable nanoshells based on the nonlocal elasticity theory,* Compos. Struct., 166 (2017), pp. 104–113.

[50] S. SAHMANI, AND M. AGHDAM, *Nonlocal strain gradient shell model for axial buckling and postbuckling analysis of magneto-electro-elastic composite nanoshells,* Compos. Part B, 132 (2018), pp. 258–274.

[51] S. SAHMANI, AND A. FATTAHI, *Small scale effects on buckling and postbuckling behaviors of axially loaded FGM nanoshells based on nonlocal strain gradient elasticity theory,* Appl. Math. Mech., 39 (2018), pp. 561–580.

[52] L. LU, L. ZHU, J. ZHAO, AND G. LIU, *A nonlocal strain gradient shell model incorporating surface effects for vibration analysis of functionally graded cylindrical nanoshells,* Appl. Math. Mech., 40(12) (2019), pp. 1695–1722.

[53] M. AREFI, AND A. ZENKOUR, *Size-dependent thermoelastic analysis of a functionally graded nanoshell,* Moder. Phys. Lett. B, (2018), 1850033.

[54] Y. LIU, AND Y. WANG, *Thermo-Electro-Mechanical Vibrations of Porous Functionally Graded Piezoelectric Nanoshells,* Nanomaterials, 9 (2019), 301.

[55] Y. ZHANG, AND F. ZHANG, *Vibration and Buckling of Shear Deformable Functionally Graded Nanoporous Metal Foam Nanoshells,* Nanomaterials, 9 (2019), 271.

[56] X. ZHAO, AND K. LEW, *A mesh-free method for analysis of the thermal and mechanical buckling of functionally graded cylindrical shell panels,* Comput. Mech., 45 (2010), pp. 297–310.

[57] D. BRUSH, AND B. ALMROTH, Buckling of Bars, Plates and Shells, New York: McGraw-Hill; 1975.

[58] M. ESLAMI, Buckling and Postbuckling of Beams, Plates, and Shells, Springer Int. Pub. AG, Gewer. 11, 6330 Cham, Switzerland; 2018.

[59] S. TIMOSHENKO, AND J. GERE, Theory of Elastic Stability, 2nd ed. New York: McGraw-Hill; 1961.